Journal of Microbiology (2022) Vol. 60, No. 1, pp. 79–88
DOI 10.1007/s12275-022-1074-7
eISSN 1976-3794
pISSN 1225-8873

Gene deletion and constitutive expression of the pectate lyase gene 1 (*MoPL1*) lead to diminished virulence of *Magnaporthe oryzae*[§]

Alex Wegner[1†], Florencia Casanova[1†], Marco Loehrer[1], Angelina Jordine[1], Stefan Bohnert[1], Xinyu Liu[2], Zhengguang Zhang[2], and Ulrich Schaffrath[1*]

[1]*Department of Plant Physiology, RWTH Aachen University, Aachen 52056, Germany*
[2]*Department of Plant Pathology, Nanjing Agricultural University, Jiangsu 210095, P. R. China*

(Received Feb 4, 2021 / Revised Aug 20, 2021 / Accepted Sep 27, 2021)

Phytopathogenic fungi are known to secrete specific proteins which act as virulence factors and promote host colonization. Some of them are enzymes with plant cell wall degradation capability, like pectate lyases (Pls). In this work, we examined the involvement of Pls in the infection process of *Magnaporthe oryzae*, the causal agent of rice blast disease. From three Pl-genes annotated in the *M. oryzae* genome, only transcripts of *MoPL1* considerably accumulated during the infection process with a peak at 72 h post inoculation. Both, gene deletion and a constitutive expression of *MoPL1* in *M. oryzae* led to a significant reduction in virulence. By contrast, mutants that constitutively expressed an enzymatic inactive version of *Mo*Pl1 did not differ in virulence compared to the wild type isolate. This indicates that the enzymatic activity of *Mo*Pl1 is responsible for diminished virulence, which is presumably due to degradation products recognized as danger associated molecular patterns (DAMPs), which strengthen the plant immune response. Microscopic analysis of infection sites pointed to an increased plant defense response. Additionally, *Mo*Pl1 tagged with mRFP, and not the enzymatic inactive version, focally accumulated in attacked plant cells beneath appressoria and at sites where fungal hyphae transverse from one to another cell. These findings shed new light on the role of pectate lyases during tissue colonization in the necrotrophic stage of *M. oryzae's* life cycle.

Keywords: *Pyricularia oryzae*, rice blast fungus, cell wall degrading enzyme (CWDE), pectate lyase, *MoPL1*, virulence factor, DAMP

Introduction

Plant pathogenic microorganisms must overcome different barriers to establish a compatible interaction with their hosts. One of the first, and possibly most crucial, barrier is the plant cell wall consisting of cellulose, non-cellulosic and pectic polysaccharides and phenolic compounds (Jones and Dangl, 2006; Keegstra, 2010; Underwood, 2012). Cellulose microfibrils crosslinked to each other by branched polysaccharides, form the framework of the primary cell wall, which additionally contains pectins that influence a variety of properties and processes like expansion, strength, porosity, adhesion, and intercellular signalling. The secondary cell wall additionally contains hemicellulose and lignin, which increase the strength of the cell wall but reduce flexibility (Houston *et al*., 2016). Because of this diverse composition, pathogens need a whole set of different cell wall degrading enzymes (CWDE) to penetrate plant cells (Quoc and Chau, 2017). Small molecules generated during the degradation process are then used by pathogens for nutrition (Jones and Dangl, 2006; Quoc and Chau, 2017). However, this ostensible benefit came along with the drawback that plants became able to sense the presence of these degradation products and interpret them as danger associated molecular patterns (DAMPs), which then in turn activate the plant immune system (Jones and Dangl, 2006; Choi and Klessig, 2016).

The fungus *Magnaporthe oryzae,* causing rice blast disease, is the most destructive threat to rice production worldwide and can infect a wide variety of grasses, such as wheat, barley, and millet. During the last decades, the rice-*M. oryzae* pathosystem has become the prime model for studying plant-fungal interactions (Dean *et al*., 2012; Saitoh *et al*., 2012). The blast fungus is hemibiotrophic and accordingly its life cycle can be divided into an initial biotrophic stage, where the fungus colonizes living host cells, and later on it switches to necrotrophy and actively kills host tissue (Ebbole, 2007). During the early plant infection process a specialized infection structure, called appressorium, is formed at the tip of a germ tube. While penetration of plant cell walls is thought to be mainly facilitated by the generation of a high turgor pressure, also the involvement of CWDE has been reported (Talbot, 2003; Ebbole, 2007; Loehrer *et al*., 2014). Once inside plant cells, bulbous invasive hyphae are formed, which spread to neighboring cells utilizing pit fields (Kankanala *et al*., 2007). Around three to four days after initial penetration, the fungus switches to necrotrophy. This is accompanied by a change in morphology from bulbous infection hyphae to thin running hyphae (Ebbole, 2007; Wilson and Talbot, 2009). In *M. oryzae*, a large number of genes (up to 1306) were predicted to encode for secreted proteins with a proposed function as virulence fac-

[†]These authors contributed equally to this work.
*For correspondence. E-mail: schaffrath@bio3.rwth-aachen.de; Tel.: +49-241-8020100
[§]Supplemental material for this article may be found at http://www.springerlink.com/content/120956.

tors (Dean *et al.*, 2005; Yoshida *et al.*, 2009; Chen *et al.*, 2013). Among them are also the CWDEs and for *M. oryzae* a total of 33 were listed (Choi *et al.*, 2013). While several were already examined for their function in virulence (Skamnioti and Gurr, 2007; Mori *et al.*, 2008; Zheng *et al.*, 2009), little is known about the pectate lyase enzyme family in *M. oryzae*.

Pectate lyases (Pls) (E.C. 4.2.2.2) cleave the α-1,4-linked glycosidic bonds between D-galacturonic acid in the main chain of pectin via a ß-elimination mechanism (van den Brink and de Vries, 2011). This gives rise to an unsaturated C4-C5 galacturonosyl residue at the nonreducing end of the polysaccharide (Yoder *et al.*, 1993; Herron *et al.*, 2000; Kanungo and Prasad, 2019). Most Pls are predicted to be transcriptionally regulated by environmental factors like pH or availability of carbon sources (Yakoby *et al.*, 2000; Miyara *et al.*, 2008). It has been recently reported that Pls are predominantly found in microorganisms living in association with plants and rarely in free-living microbes, which might account for an emergence of Pls during coevolution of microbes and plants (Levy *et al.*, 2018). Pls have been extensively studied in fungi and it was repeatedly shown that they are involved in pathogenesis (Crawford and Kolattukudy, 1987; Dean and Timberlake, 1989; Yakoby *et al.*, 2000; Cnossen-Fassoni *et al.*, 2013). Additionally, it has been reported that small oligogalacturonides produced by Pls during digestion of pectin are able to elicit plant defense reactions (van den Brink and de Vries, 2011). Despite the overwhelming research done to understand the infection process of *M. oryzae*, the function of Pls during infection remains unclear. Therefore, the aim of this study was to close this gap by characterizing the gene MGG_04348, encoding *MoPL1*, and its contribution to virulence.

Materials and Methods

The generation and validation of gene deletion mutants, mutants for complementation and mutants constitutively expressing *MoPL1*::mRFP were conducted following standard protocols. Details are given in Supplementary data Fig. S3 and Supplementary data 1.

Cultivation of fungi and plants and inoculation

The *M. oryzae* isolate Guy11 (*Mo*WT) was kindly provided by D. Tharreau (CIRAD, Montpellier, France) and cultivated on oatmeal agar (20 g/L agar, 2 g/L yeast extract, 10 g/L starch, 30 g/L oat flakes) or potato dextrose agar (PDA; Sigma Aldrich) at 23°C in the dark. For generation of conidia, isolates were incubated under fluorescent tubes with blacklight (310 to 360 nm) seven days (d) after sub-cultivation at a 16/8 h light/dark-cycle at 26°C for 7–10 days. Conidia were carefully removed with 5 ml ddH_2O using a spatula and filtered through three layers of gauze. Concentration of conidia was adjusted to 40,000 conidia/ml in a solution containing 1 g/L gelatin and 0.5 ml/L Tween 20. Barley plants cultivar Ingrid (*Hordeum vulgare* L.), kindly provided by Paul Schulze-Lefert (Max-Planck Institute for Plant Breeding Research), were cultivated at 18°C, 60% relative humidity, and at a 16/8 h light-dark cycle (210 µmol/m^2s) as described by Delventhal *et al.* (2014). Plants were inoculated by spraying the spore suspension with a compressed air atomizer, then kept first for 24 h at 24°C and 100% relative humidity in the dark before transferring to growth chamber conditions. For evaluation, the infected leaves were placed on water agar plates at 6 days post inoculation and pictures were taken using a Panasonic DMC-TZ61 camera with constant light settings to ensure consistent conditions. Disease severity was calculated by determining the infected leaf area relative to the whole leaf area using the image software Assess 2.0 (Image analysis software for plant disease quantification 2.0, https://my.apsnet.org/ItemDetail?iProductCode=43696).

RT-qPCR

For quantification of transcript abundances corresponding to *M. oryzae* genes MGG_04348, MGG_07566, MGG_05875 or barley gene *HvPR1*, samples of barley leaves inoculated with different isolates or mutants of *M. oryzae* were harvested at 12, 24, 48, 72, 96, and 120 hpi, or *in vitro* grown mycelium taken from seven-day-old oatmeal agar plates was used. For transcript abundance detection of fungal genes at early time points of the interaction (12 and 24 hpi), epidermal peels were harvested as described by Delventhal *et al.* (2014). RNA extraction was performed according to the sodium citrate extraction method (Voegele and Schmid, 2011). RNA was precipitated with 50% isopropanol, washed with 100 µl 70% ethanol and dispended in RNase free water. After DNase I treatment (DNase I, Thermo Fisher Scientific), about 200 ng RNA was utilized for cDNA synthesis with RT-Polymerase (Thermo Fisher Scientific) and HindAnchorT-primers. The cDNA samples were diluted 1:10 (v/v) with water and mixed with universal iTaq-SYBR-Green Supermix (Thermo Fisher Scientific) and corresponding primers for RT-qPCR analysis. Transcript abundances of fungal and plant genes were calculated relative to the housekeeping genes *MoACTIN* or *HvEF1*-alpha, respectively. All primers are listed in Supplementary data Table S1. RT-qPCR was conducted in an CFX96 Touch Real-Time PCR Detection System (Bio-Rad) at the following conditions: 95°C for 3 min, 40 cycles of 3 sec at 95°C and 30 sec at 60°C. The melting curves of each sample were analyzed to ensure the absence of unspecific products. Ct-values were used for evaluation using the ΔCt-method based on the procedure described in Livak and Schmittgen (2001). Transcript abundances were calculated by Expression = $2^{[Ct(reference)-Ct(target)]}$.

Microscopic evaluation of cellular infection sites

Bright-field microscopy of interaction sites from *Mo*WT, *MoPL1::mRFP*-OE and *ΔMopl1* on barley was carried out using a Leica DMR microscope (Leica Microsystems). The occurrence of autofluorescent material was recorded using the filter N2.1 513812 (515–560 nm excitation, 590 nm beam splitter and 590 nm long-pass emission). For evaluation, infected barley leaves were harvested and then fixed/destained in clearing solution (25% chloroform, 75% ethanol, 0.15% trichloracetic acid [w/v]) for one week. Fungal-plant interaction sites were grouped into the following categories: formation of an appressorium (app) without any visible plant response, a papilla visible beneath a fungal appressorium (pap), the occurrence of autofluorescent material in epidermal cells beneath an appressorium (hr), additional fluorescence in round shaped (r.fl.mc) or collapsed mesophyll cells (c.fl.mc) at sites of fungal attack (Supplementary data Fig. S7). Sites at which a par-

ticular plant cell was attacked by more than one appressorium and cells surrounding stomata were excluded from analysis.

Confocal laser scanning microscopy

Confocal laser scanning microscopy was performed using a Leica TCS SP8 Spectral Confocal Microscope (Leica Microsystems). Barley coleoptiles, prepared from plants grown for seven days in soil, were inoculated with 10 µl drops containing 10,000 spores/ml and incubated on wet filter paper in petri dishes for 72 h in the dark. The samples were excited with a wavelength of 561 nm to detect mRFP fluorescence. GFP-fluorescence was captured by exciting with 488 nm, which allows the distinction of the tagged fluorophore from autofluorescence of plant structures. The emission was monitored at 580–620 nm (mRFP) and 500–530 nm (GFP/ autofluorescence). To verify the mRFP fluorescence and to discriminate from autofluorescence of plant tissue, lambda scans were performed.

Enzyme activity measurement

The pH optimum of the pectolytic activity of *Mo*Pl1::mRFP was determined in a spectro-photometric assay using a Beckman DU 800 spectrophotometer (Beckman Coulter GmbH) as described in Bruehlmann (1995). Therefore, the increase in absorbance at 235 nm was measured in quartz glass cuvettes. An aliquot of 50 µl of the supernatant from a 14-day-old liquid culture of *MoPL1*::*mRFP*-OE (grown in complete media at 25°C, 100 rpm in a conical flask) was mixed with 1 ml polygalacturonic acid solution (1 g/L, buffered with 0.2 M glycine buffer; pH 7.0–11.0). The linear increase of absorbency in the first 4 min of measurement was used to calculate the relative pectolytic activity. To ensure the addition of the same concentration for both proteins (*Mo*Pl1::mRFP and *Mo*Pl1$^{D159A, D163A}$::mRFP), the fluorescence of the mRFP tag served as a reference. Measurement was conducted using a Jasco FP-750 Spectrofluorometer (JASCO Deutschland GmbH) and adjustment to the same rel. mRFP value by adding supernatant of *Mo*WT. The determination of enzyme activity was performed at pH 9.0.

Nicotiana benthamiana plants (Max-Planck-Institute, Cologne, Germany) were grown in VM-substrate (Balster Einheitserdewerk GmbH) and cultivated at 24°C and 16/8 h light-dark-cycle. Ten-day-old plants were transferred to new pots with ED73 substrate (Balster Einheitserdewerk GmbH) and four to six-week-old plants were used for experiments. About 0.5 ml of the supernatant from 14-days-old *M. oryzae* cultures grown in 150 ml liquid complete medium was directly infiltrated into 4–6-week-old *N. benthamiana* leaves. Supernatants derived from liquid cultures of *MoPL1*::*mRFP*-OE and *MoPL1*$^{D159A, D163A}$::*mRFP*–OE were adjusted to the same amount of recombinant protein by using the RFP fluorescence of these fusion proteins as reference. In case needed, adjustments were made using the supernatant of cultures from the *M. oryzae* wild type isolate. Inactivation of *Mo*Pl1 in the supernatant was done by heating at 90°C for 15 min. Infiltrated *N. benthamiana* leaves were incubated in petri dishes moistened with wet filter pater at 16/8 h light-dark-cycle at 20°C.

Constitutive expression of *Mo*Pl1::mRFP in *N. benthamiana*

For confirmation of secretion, the genomic sequence of *MoPL1* was amplified with primers MoPL1Fatt1 and MoPL1att2. The PCR product was first cloned into pDONR207 with Gateway BP-clonase and then into pSite4-NB using LR-clonase (Thermo Fisher Scientific), referred to as pSite4-NB::*Mo*Pl1::mRFP. This construct was transformed into *AGL*1 by heat shock. Thus, *AGL1* mediated transformation of *N. benthamiana* was performed as described in Mogga *et al.* (2016). Confocal laser scanning microscopy of infiltrated areas was conducted three days post infiltration using a set-up as described above. To substantiate observation of protein accumulation in the apoplast, plasmolysis was carried out by placing leaf sections in 0.5 M KNO_3 for vacuum infiltration.

Results

MoPL1 encodes a secreted pectate lyase that macerates plant tissue

A BLAST analysis using the NCBI data base (https://www.ncbi.nlm.nih.gov/) revealed three genes in the *M. oryzae*

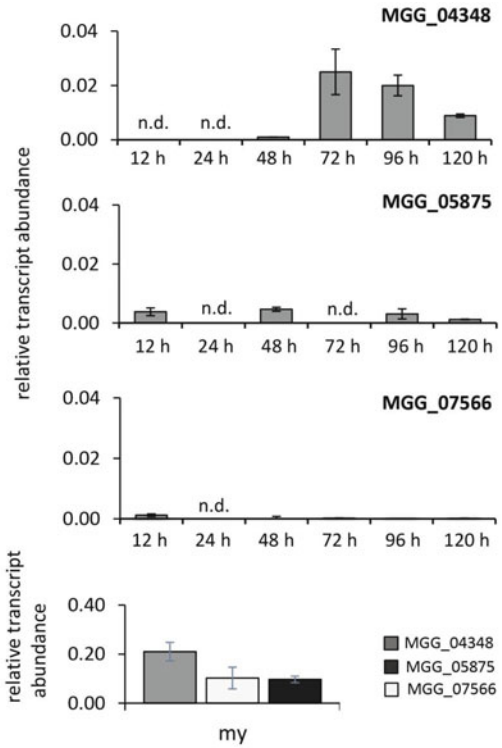

Fig. 1. Transcript abundances of pectate lyases from *M. oryzae* during infection and in mycelia. Seven days after germination primary leaves of the barley cultivar Ingrid *Mlo* were inoculated with conidia of *M. oryzae* isolate Guy11. Total RNA was extracted from three inoculated leaves harvested at indicated time points or from *in vitro* grown mycelia (my) seven days after sub-culturing. Transcript abundances of the genes MGG_04348 (*MoPL1*), MGG_07566 and MGG_05875 were determined using RT-qPCR and calculated relative to the gene *MoACTIN* (MGG_03982). Columns represent mean values and standard errors from three technical replicates. Experiments were repeated in triple with similar results. n.d., no detectable transcript abundance.

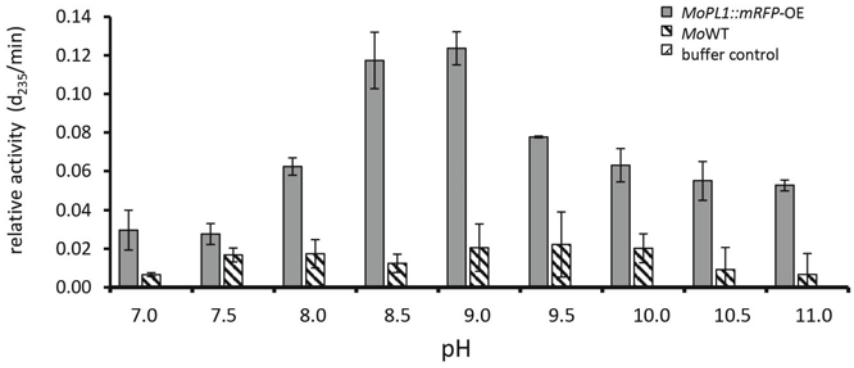

Fig. 2. Spectro-photometric of the pectolytic activity of *Mo*Pl1 at different pH. One of the *M. oryzae* mutants expressing *MoPL1::mRFP* (*MoPL1::mRFP*-OE) was grown in liquid culture and the supernatant was collected after 14 days. The supernatant was mixed with glycine-buffer solutions with different pH values, which contained polygalacturonic acid as substrate. The pectolytic activity was recorded by measurement of the produced unsaturated C4-C5 galacturonosyl residue using the change in absorbance at 235 nm over time (d_{235}/min). Same was done using the supernatant of a wild type culture (*Mo*WT) and heat inactivated supernatant (10 min, 90°C) of *MoPL1::mRFP*-OE. Columns represent mean values and standard errors from three technical replicates. The experiment was repeated three times with similar results.

70–15 genome encoding for proteins containing a domain characteristic for pectate lyases (Pls), which is in agreement with literature data (Quoc and Chau, 2017). For the determination of gene expression profiles of these genes, RNA was extracted from barley leaves at different time points after inoculation with a virulent isolate of *M. oryzae*. RT-qPCR analyses showed considerable transcript accumulation only for gene MGG_04348 (*MoPL1*) with a peak at 72 h post inoculation (hpi) (Fig. 1). By contrast, for gene MGG_07566 and MGG_05875 no or only a marginal accumulation of transcripts was detected (Fig. 1). Remarkably, transcripts of *MoPL1* were not detectable during the biotrophic stage of the *M. oryzae* infection process at 12 and 24 hpi. A comparison with published transcriptome studies revealed the same tendencies for gene expression patterns of all three Pls during the infection process (Dong *et al.*, 2015; Shimizu *et al.*, 2019; Jeon *et al.*, 2020). Transcripts of all three Pls were also detected *in vitro* in mycelia grown on oatmeal agar (Fig. 1).

To confirm the prediction that *Mo*Pl1 is secreted, *Agrobacterium tumefaciens* mediated transformation was carried out to achieve a transiently expression of *MoPL1::mRFP* in *Nicotiana benthamiana* epidermal cells. Using confocal laser scanning microscopy, the mRFP fluorescence was detected in the apoplastic space surrounding epidermal plant cells (Supplementary data Fig. S1). Allocation of the fluorescence to the apoplast was underpinned after applying plasmolysis, which confirmed that the gene MGG_04348 encodes a secreted protein.

Verification that the gene MGG_04348 in fact encodes a protein with Pl activity was done by generating mutants of *M. oryzae* that constitutively expressed a version of the protein fused to monomeric red fluorescent protein (mRFP) (*MoPL1 ::mRFP*-OE). Because *Mo*Pl1::mRFP is secreted (Supplementary data Fig. S1), the supernatant of a liquid culture from

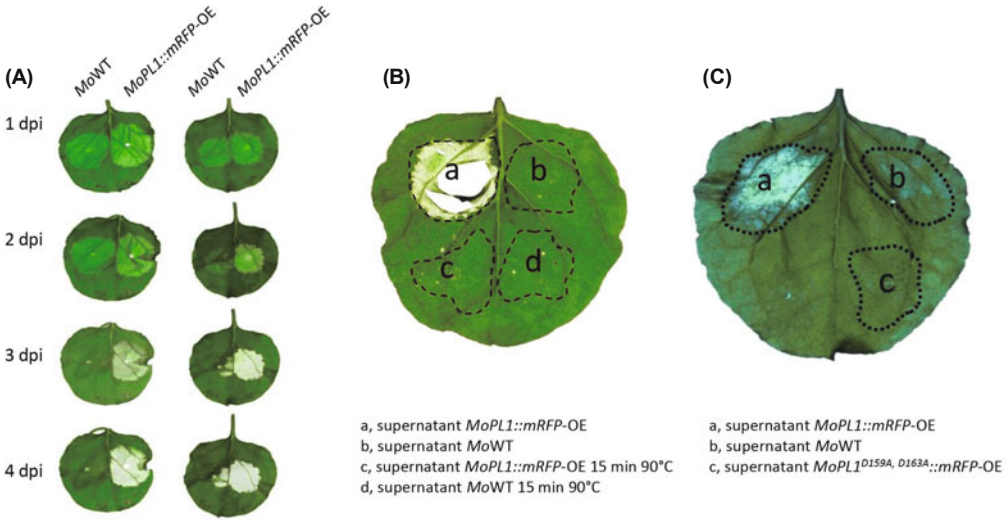

Fig. 3. Infiltration of supernatants of liquid cultures from different *M. oryzae* mutants or wild type isolates in leaves of *Nicotiana benthamiana*. (A) The supernatant of 14-day-old liquid cultures of a *M. oryzae* wild type isolate (*Mo*WT) and a mutant constitutively expressing *Mo*Pl1::mRFP (*MoPL1::mRFP*-OE) were infiltrated into leaves of 4-week-old *N. benthamiana* plants. Each leaf was infiltrated on the left and right side with the supernatant of *Mo*WT or *MoPL1::mRFP*-OE as indicated. Representative pictures of two leaves, of a minimum of eight leaves per experiment, were taken from one to four days after infiltration. The experiment was repeated in quadruple with similar results. (B) Supernatants of liquid cultures from *Mo*WT or *MoPL1::mRFP*-OE were heated to 90°C for 15 min prior to infiltration into *N. benthamiana* leaves. Pictures of representative leaves were taken four days after infiltration. Dashed lines indicate the infiltrated leaf area. The experiment was repeated twice with similar result. (C) The supernatant of 14-day-old liquid cultures of *Mo*WT or *MoPL1::mRFP*-OE or a mutant expressing a pectolytic inactive version of *Mo*PL1 (*MoPL1*$^{D159A, D163A}$*::mRFP*-OE) were infiltrated into *N. benthamiana* leaves. After four days pictures of representative leaves were taken. The experiment was done once with a total of eight leaves. Dashed lines indicate infiltrated areas.

MoPL1::*mRFP*-OE was collected 14 days after sub-culturing and could directly be used for pectolytic activity measurement by adding polygalacturonic acid. Spectro-photometrical determination of the change in absorbance at 235 nm, corresponding to an increase of the produced unsaturated hexenuronic acid, confirmed the protein encoded by gene MGG_04348 as a functional Pl (Fig. 2). By varying the pH of the enzyme cocktail, an optimum for the enzyme activity in the range between pH 8.5 and 9.5 was determined (Fig. 2).

To analyze the capacity of *Mo*Pl1 to degrade plant cell walls, the supernatants of a liquid culture of the *M. oryzae* wild type isolate Guy11 (*Mo*WT) and the mutant *MoPL1*::*mRFP*-OE were collected and infiltrated into *N. benthamiana* leaves (Fig. 3). Two days after infiltration a pronounced tissue maceration was observed on leaves treated with the supernatant of the mutant but not at sites where the supernatant of *Mo*WT was used. This difference became further manifested three and four days after infiltration (Fig. 3A). Only the high pectolytic activity of *MoPL1*::*mRFP*-OE, and not the lower activity of *Mo*WT, was sufficient to macerate the plant tissue (Supplementary data Fig. S2). Heat treatment of the supernatant of *MoPL1*::*mRFP*-OE prior to infiltration abolished the effect on tissue maceration, indicating that correct protein folding, i.e. a functional enzyme, is mandatory (Fig. 3B).

Deletion of *MoPL1* and the constitutive expression of *MoPL1*::*mRFP* both lead to reduced virulence of *M. oryzae*

To further characterize *MoPL1*, its impact on the infection process was evaluated. Therefore, mutants with a gene deletion (*ΔMopl1*) and mutants constitutively expressing *MoPL1*::*mRFP* (*MoPL1*::*mRFP*-OE) were generated. All independently obtained mutants were confirmed by PCR (Supplementary data Fig. S3) and additionally, transcript abundances were determined by RT-qPCR. The latter revealed no detectable transcripts of *MoPL1* in *ΔMopl1* and a strong accumulation of transcripts in *MoPL1*::*mRFP*-OE, ranging from a 4- to 20-fold increase in *in vitro* grown mycelia compared to *Mo*WT (Supplementary data Fig. S3C). For further characterization of the mutants, mycelial growth on PDA was recorded, revealing a slight decrease (30%) of the colony area of *ΔMopl1* compared to *Mo*WT, whereas the constitutive expression of *MoPL1*::*Mrfp* had no impact (Supplementary data Fig. S4). A similar tendency on colony growth was observed on minimal media containing polygalacturonic acid as the sole carbon source (Supplementary data Fig. S4).

The impact of *Mo*Pl1 on virulence was determined by inoculation of mutants and the wild type isolate on primary leaves of barley *cv.* Ingrid. Macroscopic evaluation of disease severity seven days after inoculation revealed a clear reduction in lesion density for *ΔMopl1* and *MoPL1*::*mRFP*-OE (Fig.

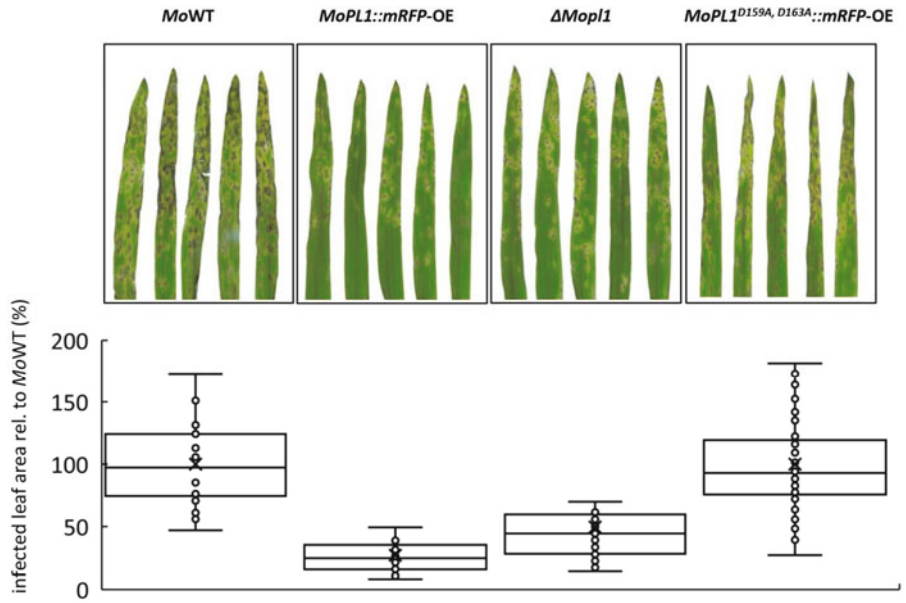

no. of leaves	107	34	29	71
no. of exp.	7	3	3	3
p-value		5.67E-17	1.18E-07	not significant

Fig. 4. Infection phenotypes of fungal mutants and the wild type isolate on barley leaves. Primary leaves of barley cultivar Ingrid *Mlo* were inoculated with conidia of the *M. oryzae* wild type isolate Guy 11 (*Mo*WT), the gene deletion mutant (*ΔMopl1*), and mutants constitutive expressing *MoPL1*::mRFP (*MoPL1*::*mRFP*-OE) or a with constitutive expressing a pectolytic inactive version of *Mo*Pl1 tagged with mRFP (*MoPL1*$^{D159A,\ D163A}$::*mRFP*-OE). Leaves were photographed seven days post inoculation. Disease severities were calculated for each infected leaf using the image software Assess 2.0. Representative pictures of leaves are shown for each interaction and disease severity data are shown as box-plot below each image. To compare data from different experiments values are calculated relative to *Mo*WT which was set to 100% in each experiment. For statistical analysis, each mutant was compared to *Mo*WT using T-test and p-values for significant differences, number (no.) of independent biological experiments (exp.) and leaves analyzed over all experiments are given below each bar.

4). Pictures of all inoculated leaves were taken and digital imaging-based scoring substantiated the evaluation by eye. Thus, an almost 50% and 75% reduction in disease severity was recorded for *ΔMopl1* and *MoPL1::mRFP*-OE, respectively (Fig. 4; Supplementary data Fig. S9). However, size and shape of fully developed disease symptoms did not differ between mutants and wild type isolate. An in locus complementation with *MoPL1::mRFP*, which replaced the selection marker in the *ΔMopl1* mutant (Supplementary data Fig. S3), confirmed that the mRNA fusion protein is functionally similar to the wild type enzyme regarding the infection phenotype (Supplementary data Fig. S10).

It is known from other pathosystems, that degradation products of pectate lyases may act as alert signals for the plant immune system, and consequently reduce the infection success of a pathogen (Hou *et al*., 2019). We challenged this hypothesis for the barley/*M. oryzae* pathosystem by generating mutants that expressed an inactive version of the enzyme. Putative polygalacturonic acid binding sites of *Mo*Pl1 were identified by alignment and comparison to well-characterized Pls (Yoder *et al*., 1993) (Supplementary data Fig. S5). Thus, using site-directed mutagenesis two substitutions with alanine (D159A and D163A) were introduced at Ca^{2+} binding sites, which are predicted to be crucial for substrate binding (Yoder *et al*., 1993). The respective construct for constitutive expression of this inactive version of the protein (Supplementary data Fig. S3) was introduced in *Mo*WT by protoplast transformation as described in Leisen *et al*. (2020) and confirmed by PCR analysis. The corresponding mutants were named *MoPL1*$^{D159A,\ D163A}$*::mRFP*-OE. RT-qPCR revealed different transcript abundances in *in vitro* grown mycelia, with a maximum of 27 fold increase in different independent clones of *MoPL1*$^{D159A,\ D163A}$*::mRFP*-OE compared to the *Mo*WT (Supplementary data Fig. S3). Spectro-photometrical measurement of the supernatant of these mutants grown in liquid culture revealed only a slight background Pl activity, which originated from further pectolytic enzymes of the fungus (Supplementary data Figs. S2 and S6). Comparing mutants that constitutively express either the native or mutated version of *Mo*Pl1::mRFP revealed no enhanced enzyme activity for the latter mutants, confirming that the mutated version of the protein is enzymatically inactive (Supplementary data Fig. S2). Analysis done with I-TASSER, a tool to calculate protein structures, suggested no structural differences in folding between the recombinant protein *Mo*Pl1$^{D159A,\ D163A}$::mRFP and the wild type version of the enzyme (Supplementary data Fig. S5). Comparison of mycelial growth between mutants *MoPL1*$^{D159A,\ D163A}$*::mRFP*-OE and *Mo*WT on PDA or minimal medium revealed no obvious penalties due to the mutations (Supplementary data Fig. S4). Inoculation experiments disclosed that the lesion area of infected barley leaves inoculated with *MoPL1*$^{D159A,\ D163A}$*::mRFP*-OE did not differ from *Mo*WT (Fig. 4). Thus, a reduction in virulence, as observed for the *MoPL1::mRFP*-OE mutant, did not occur when genes were expressed encoding for enzymatic inactive versions of the protein.

During measurement of pectolytic activity in different mutants it was further observed that *ΔMopl1* had a residual enzymatic activity compared to *Mo*WT (Supplementary data Fig. S2). Inquiring for an explanation, RT-qPCR analysis was performed with isolates grown in 14-day-old liquid culture revealing that transcripts of MGG_04348 (*MoPL1*) were not detectable in the wild type nor in the deletion mutant (Supplementary data Fig. S6). Instead, transcripts specific for genes MGG_05875 and MGG_07566 were recorded. Therefore, it seems that deletion of the gene *MoPL1* was compensated in the mutant *ΔMopl1* by an up-regulation of the other two

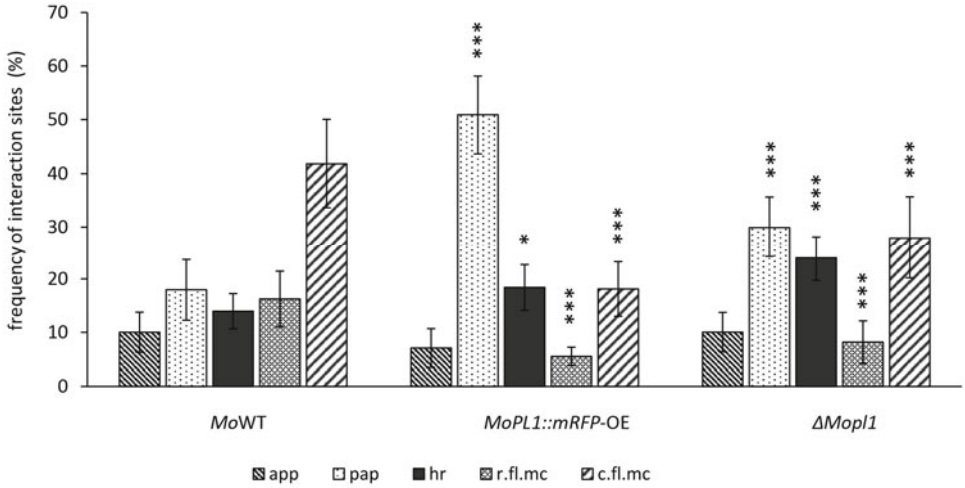

Fig. 5. Microscopic evaluation of infection sites of *M. oryzae* wild type and mutant isolates on barley plants. Interaction phenotypes of barley cells with different *M. oryzae* genotypes. Primary leaves of barley plants cv. Ingrid *Mlo* were inoculated with the wild type (*Mo*WT), gene deletion mutant (*ΔMopl1*) and a mutant constitutively expressing the mRFP tagged pectate lyase (*MoPL1::mRFP*-OE) and harvested 72 h after inoculation. After destaining, leaves were evaluated by bright-field and epi-fluorescence microscopy. Interaction sites were grouped into different categories, depending on the absence or presence of fluorescence of plant cells attacked by the fungus. Categories are defined as follows: no fluorescence at the site of appressorium formation (app), a fluorescent halo (papilla) beneath fungal appressorium (pap), the occurrence of autofluorescent material in epidermal cells beneath an appressorium (hr), fluorescence of round shaped, intact (r.fl.mc) or collapsed (c.fl.mc) mesophyll cells in direct contact to attacked epidermal cells. Columns represent mean values and standard errors from three combined independent experiments. For each fungal genotype four to five leaves with a total of 50–80 interaction sites per leaf were analyzed. Significant differences ($p < 0.1$; $p < 0.01$; $p < 0.001$ confidence were indicated by *, **, and *** respectively) for each category were determined by Student's T-test between each single mutants and the wild type isolate.

pectate lyase genes. In consequence, the residual pectate lyase activity in *ΔMopl1* must be caused by the enzymes encoded by the latter two genes.

Microscopical analysis hints to different function for *MoPL1* during infection

For a better understanding of the reduced virulence phenotype observed for *ΔMopl1* and *MoPL1::mRFP*-OE, infected leaves were analyzed by bright-field and epifluorescence microscopy. After removal of chlorophyll, individual interaction sites, for example plant cells attacked by a fungal appressorium, were examined for the presence or absence of autofluorescent material and grouped into different categories. These microscopic samples were first screened using bright field microscopy to localize appressoria and subsequently the determination of auto-fluorescence was enabled by epifluorescent light (Supplementary data Fig. S7). Previously, it had been shown that the deposition of auto-fluorescent material beneath an appressorium or/and strong epifluorescence at cell walls of attacked epidermal cells is correlated with a stop of fungal invasion (Jarosch *et al.*, 2003, 2005). Deposition of auto-fluorescent material close to collapsed mesophyll cells, by contrast, was correlated with successful pathogen invasion. Leaf samples from plants inoculated with wild type or mutant strains, were harvested 72 hpi and analyzed by quantitative microscopy (Fig. 5). A significant increase in the categories "papilla" and "hypersensitive response" was observed between *Mo*WT and *ΔMopl1*, both associated with a stop of fungal invasion during penetration, raised from 18% to 30% and 14% to 24%, respectively. By contrast, the category "collapsed fluorescent mesophyll cells", correlated with successful pathogen invasion into the mesophyll, decreased from 42% to 28% (Fig. 5). Taken together, these observations indicate a correlation between the deletion of *MoPL1* and a reduction in penetration success. Regarding *MoPL1::mRFP*-OE the category "papilla" increased significantly from 18% to 52% in comparison to *Mo*WT (Fig. 5). A lower increase was observed for the category "hypersensitive response." These data revealed an early block of invasion for both types of mutants, which is even more pronounced in case of the *MoPL1::mRFP*-OE mutant.

*Mo*Pl1::mRFP localizes at plasmodesmata used for cell-to-cell movement of infection hyphae

Confocal microscopy was applied to trace the accumulation of *Mo*Pl1::mRFP in constitutively expressing mutants. Conidia of *MoPL1::mRFP*-OE were inoculated on coleoptiles of seven-day-old barley plants and analyzed at 72 hpi (Fig. 6). Coleoptiles were used because the lack of chlorophyll makes them an ideal tissue for fluorescence microscopy. Cells invaded by hyphae showed a pronounced accumulation of *Mo*Pl1::mRFP at 72 hpi, verifying that the fusion protein was secreted by

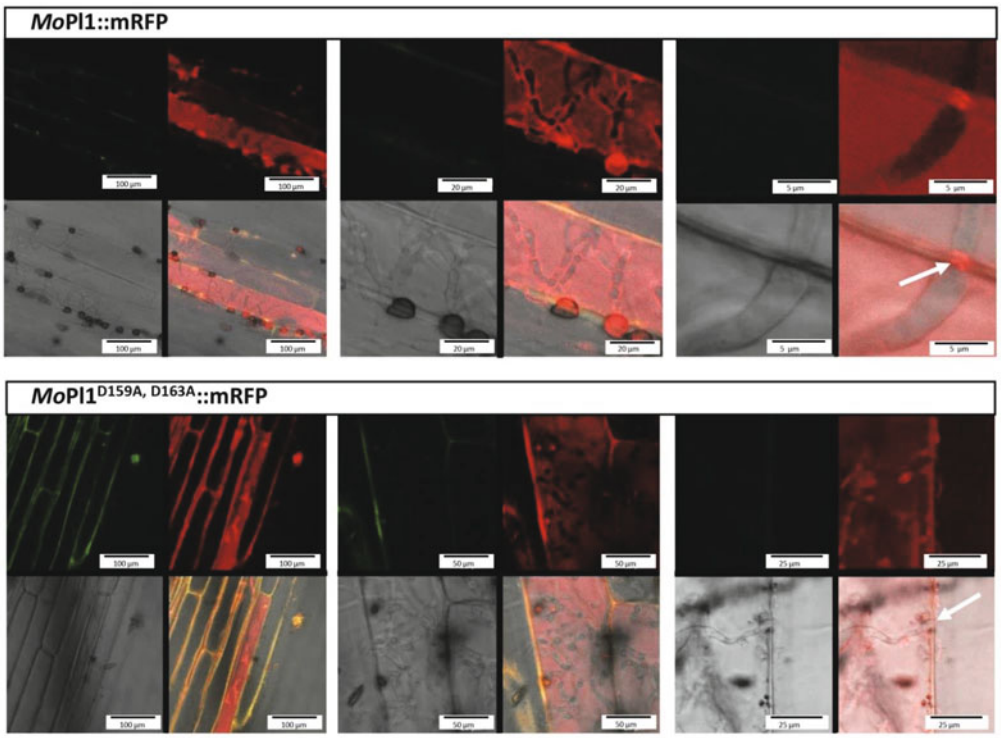

Fig. 6. Localization studies of *Mo*Pl1::mRFP and the enzymatic inactive version *Mo*Pl1$^{D159A, D163A}$::mRFP. Seven-day-old coleoptiles of barley plants were drop-inoculated with conidia of *M. oryzae* mutants *MoPL1::mRFP*-OE and *MoPL1*$^{D159A, D163A}$*::mRFP*-OE. Confocal laser-scanning microscopy was carried out 72 h post inoculation using Leica TCS SP8 confocal microscope. For each mutant, three infection sites are shown at different magnifications. Each infection site was recorded with different light excitations shown as composite Figure: GFP-channel, 488 nm (top left), mRFP-channel, 561 nm (top right), bright field (bottom left) and merged channel (bottom right). Autofluorescence, detected in the GFP channel, is shown as yellow color in overlay composition. To confirm mRFP fluorescence and distinguish from autofluorescence, lambda scans were performed. *Mo*Pl1::mRFP was detected in the plant cell cytoplasm and at sites of hyphal transversion from infected to adjacent cells (marked with arrow). In mutant *MoPL1*$^{D159A, D163A}$*::mRFP*-OE no accumulation of the enzymatic inactive fusion-protein could be observed at hyphal transversion sites.

MoPL1::*mRFP*-OE during infection. These infected cells were apparently dead because they did not respond to plasmolysis. Investigation of infection sites at a higher magnification revealed that the fusion protein accumulated focally beneath the contact zone of appressoria and plant cell walls and, interestingly, at sites where fungal hyphae spread from one to another cell (Fig. 6, upper row of images). The accumulation of *Mo*Pl1::mRFP at these different sites during infection is in agreement with the two modes of action postulated for the *MoPL1*::*mRFP*-OE mutant, i.e. enhancing penetration resistance and diminishing mesophyll invasion, as suggested by data obtained by quantitative microscopy. By contrast no focal accumulation of the fusion protein at none of the before mentioned sites could be detected after inoculation of coleoptiles with *MoPL1*$^{D159A,\ D163A}$::*mRFP*-OE, indicating that pectolytic activity or the replaced Ca^{2+} binding sites are necessary for reallocation of *Mo*Pl1.

Constitutive expression of *MoPL1*::*mRFP* enhances the accumulation of transcripts of the plant defense gene *HvPR1*

To detect putative differences in the plant response during infection with different mutants of *M. oryzae*, the accumulation of transcripts of *HvPR*1 (*Hordeum vulgare* pathogen-related protein 1) were quantified. Therefore, conidia of *Mo*WT, *MoPL1* ::*mRFP*-OE and *ΔMopl1* were inoculated on seven-day-old barley plants and samples for RNA extraction were harvested daily over a period of five days. These samples were prepared for RT-qPCR analysis. At the first and second day after inoculation transcripts for *HvPR1* were rarely detectable. At 72 hpi *HvPR1* transcript abundance was similar in plants inoculated with *Mo*WT and *ΔMopl1* and did not increase during the next two days (Supplementary data Fig. S8). A similar level of *HvPR1* transcript abundance was found in plants inoculated with *MoPL1*::*mRFP*-OE not before 96 hpi. However, in the later interaction a further, pronounced increase (2.5×) in transcript abundance was observed at 120 hpi in plants inoculated with *MoPL1*::*mRFP*-OE (Supplementary data Fig. S8).

Discussion

Pectate lyases of fungi are members of multigene families and in the *M. oryzae* genome three Pls are annotated (Quoc and Chau, 2017). A first clue, which of these Pls is most crucial for the infection of *M. oryzae* became apparent after RT-qPCR analyses. Thus, only the abundance of transcripts related to gene MGG_04348, referred to as *MoPL1*, increased to a considerable amount at 72 to 120 h post inoculation (hpi) (Fig. 1). By contrast, transcripts specific for the two other Pls were only marginally detected in leaves of barley plants between 12 and 120 hpi. RT-qPCR analyses with a *MoPL1* gene deletion mutant revealed that in absence of the latter gene a transcriptional upregulation of the other two Pl coding genes occurs, possibly to compensate the lack of this enzyme (Supplementary data Fig. S6). BLAST analysis with *Mo*Pl1 as query revealed that proteins with high sequence identity were only present in plant-associated microorganisms like *Colletotrichum* spp., *Gaeumannomyces tritici* and *Fusarium* spp. This is in accordance with the prediction that Pls are one of a few examples of proteins predominantly found in plant-associated microbes (Levy *et al.*, 2018). The coding sequence of *MoPL1* starts with a predicted secretion signal. After addition of a fluorophore (*MoPL1*::*mRFP*) secretion was confirmed in transiently transformed epidermal cells of *N. benthamiana* (Supplementary data Fig. S1). After secretion was verified, we could use the supernatant of liquid cultures to directly measure enzymatic activity. The fact that the protein *Mo*Pl1 ::mRFP has Pl enzymatic activity was proven by generating a mutant that constitutively expressed this fusion-protein (*MoPL1*::*mRFP*-OE) in a spectro-photometric assay with polygalacturonic acid as substrate (Fig. 2). In this way also the pH-optimum of the enzyme was found to range between 8.5 and 9.5.

Plant immune responses are generally associated with a modulation of the extracellular pH and alkalinization is postulated as a result from inhibition of plasma membrane H^+-ATPases (Elmore and Coaker, 2011). According to the alkaline pH optimum determined for *Mo*Pl1 (Fig. 2), it is very likely that the enzyme also functions in the apoplast after induction of immune responses. Furthermore, it has been demonstrated for a Pl from *Aspergillus nidulans* that the increase in alkalinization of the medium accelerated the secretion of the enzyme (Yakoby *et al.*, 2000). Thus, a positive feed-back loop can be predicted for *Mo*Pl1 secretion into the apoplast during the necrotrophic stage of the pathogen's life cycle, which is in accordance with the peak of transcript accumulation found around 72 hpi (Fig. 1). After infiltration of a solution containing *Mo*Pl1::mRFP into *N. benthamiana* leaves, tissue maceration was observed between one and four days after treatment (Fig. 3). Heat inactivation, or infiltration with versions of the enzyme containing a modified substrate binding pocket, proved that this phenotype strictly depends on the enzymatic activity of *Mo*Pl1.

Next, it was investigated whether or not *Mo*Pl1 contributes to virulence. Therefore, a mutant of *M. oryzae* was generated, in which *MoPL1* was replaced by a resistance marker (Hyg^R) (Supplementary data Fig. S3). Inoculation of barley plants with conidia from this gene deletion mutant (*ΔMopl1*) resulted in a significant reduction of infected leaf area of about 50% in comparison to the wild type (Fig. 4). Using microscopy to investigate plant cell responses to pathogen attack, we could reveal that reduced disease severity caused by *ΔMopl1* was correlated with a higher rate of penetration attempts counterattacked by the formation of papilla or deposition of autofluorescent material in epidermal plant cells (Fig. 5). These cellular reactions are known to be correlated with diminished or delayed penetration of *M. oryzae* on barley plants (Jarosch *et al.*, 2005). Concomitantly, the rate of infection sites showing collapsed mesophyll, an indication for successful pathogen proliferation, was reduced in barley plants attacked by the *ΔMopl1* mutant in comparison to *Mo*WT. Similarly, in *Colletotrichum lindemuthianum* the deletion of a Pl in the mutant *pecCL1* led to less anthracnosis disease symptoms (Cnossen-Fassoni *et al.*, 2013). It was reported for many organisms that a deletion of Pl affects growth on artificial media (Guo *et al.*, 1995; Yakoby *et al.*, 2000; Miyara *et al.*, 2008). Accordingly, *ΔMopl1* showed slightly reduced mycelial growth on agar plates containing pectate (Supplementary data Fig. S4). This might point to a compromised nutrient uptake in the mutant. Hence, it could not be excluded that reduced virulence of *ΔMopl1* is, at least in part, caused by impaired up-

take of Pl digestion products. If this is the case, one would assume that a mutant constitutively expressing *Mo*Pl1 would be more virulent than a wild type isolate. Surprisingly, quite the contrary was true. Inoculation of barley plants with a mutant, in which a fusion protein *Mo*Pl1::mRFP is expressed under control of a strong constitutive promoter (*MoPL1::mRFP*-OE), also showed less disease symptoms compared to *Mo*WT and even less than *ΔMopl1* (Fig. 4). This on first glance contradictory result could be explained by the ability of plants to recognize Pl degradation products, which act as DAMPs and activate the plant immune system (Hou *et al*., 2019). In this scenario, the strong constitutive expression of *MoPL1::mRFP* leads to a burst of a DAMP, acceleration of immune responses and, in consequence, reduced success of the pathogen to colonize barley. Conclusively, inoculation of barley plants with a mutant expressing an inactive version of the *Mo*Pl1 protein was conducted, and thus did not lead to excess DAMP deliberation, revealing no differences in virulence compared to the wild type (Fig. 4). Therefore, PAMP activity of the *Mo*Pl1 protein can be excluded. It has to be taken into consideration that the wild type *Mo*Pl1 protein is still present in both types of mutants (*MoPL1::mRFP*-OE and those with the enzymatic inactive version) and accordingly a background Pl activity was measured (Supplementary data Fig. S2). The acceleration of defense-associated responses of barley inoculated with *MoPL1::mRFP*-OE became also obvious by the strong induction of *HvPR1* expression at 120 hpi compared to wild type and gene deletion mutant (Supplementary data Fig. S8).

The observation of reduced virulence for *MoPL1::mRFP*-OE already was reported in a previous study (Wang and Valent, 2009), however no in-depth analysis on the underlying mechanisms was performed. Therefore, we analyzed the cellular interaction sites of barley plants inoculated with *MoPL1::mRFP*-OE. A similar increase in incidences allocated to the category "papilla" associated with reduced penetration efficiency was revealed as observed previously for *ΔMopl1* (Fig. 5). However, for *MoPL1::mRFP*-OE the rate of interaction sites grouped in the category collapsed mesophyll were extremely low, indicating a successful block of fungal penetration before transition of infection hyphae to the mesophyll. Confocal imaging of coleoptiles from barley plants inoculated with *MoPL1::mRFP*-OE led to the observation of a focal accumulation of the fusion protein beneath appressoria and at sites of the cell wall where fungal hyphae traverse from one to another cell. It was reported by Kankanala *et al.* (2007) that *M. oryzae* transverses through plasmodesmata from an infected cell to adjacent cells. Based on the dual sites at which *Mo*Pl1::mRFP accumulated, we suspect that *Mo*Pl1 may contribute to success of penetration and to cell-to-cell movement of infection hyphae. Further, it is evident that the observed focal accumulation of *Mo*Pl1::mRFP at both infection sites is strictly dependent on the enzymatic function of *Mo*Pl1 because imaging of barley coleoptiles infected with *MoPL1*$^{D159A,\ D163A}$*::mRFP*-OE did not show this pattern (Fig. 6). Considering the transcript abundance peak at 72 h and its absence in the biotrophic stage, it can also be speculated that stringent regulation of *MoPL1* is crucial for full virulence of the pathogen. The function of *Mo*Pl1 during invasive growth of *M. oryzae* was not reported before.

Acknowledgements

The authors would like to thank Matthias Hahn for hosting AW during an internship and guidance in fungal transformation. Asaf Levy is kindly acknowledged for sharing data in advance of publication. Work of AW and FC was financed by RWTH Aachen University scholarships for Doctoral Students.

Conflict of Interest

The authors declare that they have no competing interests.

Author Contributions

AW and FC performed most of the experiments, interpreted results and drafted the manuscript. AJ did experiments related to RT-qPCR analyses. ML and SB designed experiments and helped in the interpretation of the results. XL and ZZ contributed to the final version of the manuscript. US designed experiments and finalized the manuscript. All coauthors read and approved the final version.

Data Availability

The data that support the findings of this study are available from the corresponding author upon reasonable request.

References

Bruehlmann, F. 1995. Purification and characterization of an extracellular pectate lyase from an *Amycolata* sp. *Appl. Environ. Microbiol.* **61**, 3580–3585.

Chen, C., Lian, B., Hu, J., Zhai, H., Wang, X., Venu, R.C., Liu, E., Wang, Z., Chen, M., Wang, B., *et al.* 2013. Genome comparison of two *Magnaporthe oryzae* field isolates reveals genome variations and potential virulence effectors. *BMC Genomics* **14**, 887.

Choi, J., Kim, K.T., Jeon, J., and Lee, Y.H. 2013. Fungal plant cell wall-degrading enzyme database: a platform for comparative and evolutionary genomics in fungi and Oomycetes. *BMC Genomics* **14**, S7.

Choi, H.W. and Klessig, D.F. 2016. DAMPs, MAMPs, and NAMPs in plant innate immunity. *BMC Plant Biol.* **16**, 232.

Cnossen-Fassoni, A., Bazzolli, D.M.S., Brommonschenkel, S.H., Fernandes de Araújo, E., and de Queiroz, M.V. 2013. The pectate lyase encoded by the *pecCl*$_1$ gene is an important determinant for the aggressiveness of *Colletotrichum lindemuthianum*. *J. Microbiol.* **51**, 461–470.

Crawford, M.S. and Kolattukudy, P.E. 1987. Pectate lyase from *Fusarium solani* f. sp. *pisi*: Purification, *in vitro* translation of the mRNA, and involvement in pathogenicity. *Arch. Biochem. Biophys.* **258**, 196–205.

Dean, R.A., Kan, J.A.L., Pretorius, Z.A., Hammond-Kosack, K.E., Di Pietro, A., Spanu, P.D., Rudd, J.J., Dickman, M., Kahmann, R., Ellis, J., *et al.* 2012. The Top 10 fungal pathogens in molecular plant pathology. *Mol. Plant Pathol.* **13**, 414–430.

Dean, R.A., Talbot, N.J., Ebbole, D.J., Farman, M.L., Mitchell, T.K., Orbach, M.J., Thon, M., Kulkarni, R., Xu, J.R., Pan, H., *et al.* 2005. The genome sequence of the rice blast fungus *Magnaporthe grisea*. *Nature* **434**, 980–986.

Dean, R.A. and Timberlake, W.E. 1989. Production of cell wall-degrading enzymes by *Aspergillus nidulans*: A model system for fungal pathogenesis of plants. *Plant Cell* **1**, 265–273.

Delventhal, R., Falter, C., Strugala, R., Zellerhoff, N., and Schaffrath, U. 2014. Ectoparasitic growth of *Magnaporthe* on barley triggers expression of the putative barley wax biosynthesis gene *CYP96B22* which is involved in penetration resistance. *BMC Plant Biol.* **14**, 26.

Dong, Y., Li, Y., Zhao, M., Jing, M., Liu, X., Liu, M., Guo, X., Zhang, X., Chen, Y., Liu, Y., *et al.* 2015. Global genome and transcriptome analyses of *Magnaporthe oryzae* epidemic isolate 98-06 uncover novel effectors and pathogenicity-related genes, revealing gene gain and lose dynamics in genome evolution. *PLoS Pathog.* **11**, e1004801.

Ebbole, D.J. 2007. *Magnaporthe* as a model for understanding host-athogen interactions. *Annu. Rev. Phytopathol.* **45**, 437–456.

Elmore, J.M. and Coaker, G. 2011. The role of the plasma membrane H^+-ATPase in plant-microbe interactions. *Mol. Plant* **4**, 416–427.

Guo, W., González-Candelas, L., and Kolattukudy, P.E. 1995. Cloning of a novel constitutively expressed pectate lyase gene *pelB* from *Fusarium solani* f. sp. *pisi* (*Nectria haematococca*, mating type VI) and characterization of the gene product expressed in *Pichia pastoris*. *J. Bacteriol.* **177**, 7070–7077.

Herron, S.R., Benen, J.A., Scavetta, R.D., Visser, J., and Jurnak, F. 2000. Structure and function of pectic enzymes: Virulence factors of plant pathogens. *Proc. Natl. Acad. Sci. USA* **97**, 8762–8769.

Hou, S., Liu, Z., Shen, H., and Wu, D. 2019. Damage-associated molecular pattern-triggered immunity in plants. *Front. Plant Sci.* **10**, 646.

Houston, K., Tucker, M.R., Chowdhury, J., Shirley, N., and Little, A. 2016. The plant cell wall: a complex and dynamic structure as revealed by the responses of genes under stress conditions. *Front. Plant Sci.* **7**, 984.

Jarosch, B., Collins, N.C., Zellerhoff, N., and Schaffrath, U. 2005. *RAR1*, *ROR1*, and the actin cytoskeleton contribute to basal resistance to *Magnaporthe grisea* in barley. *Mol. Plant Microbe Interact.* **18**, 397–404.

Jarosch, B., Jansen, M., and Schaffrath, U. 2003. Acquired resistance functions in *mlo* barley, which is hypersusceptible to *Magnaporthe grisea*. *Mol. Plant Microbe Interact.* **16**, 107–114.

Jeon, J., Lee, G.W., Kim, K.T., Park, S.Y., Kim, S., Huh, A., Chung, H., Lee, D.Y., Kim, C.Y., and Lee, Y.H. 2020. Transcriptome profiling of the rice blast fungus *Magnaporthe oryzae* and its host *Oryza sativa* during infection. *Mol. Plant Microbe Interact.* **33**, 141–144.

Jones, J.D.G. and Dangl, J.L. 2006. The plant immune system. *Nature* **444**, 323–329.

Kankanala, P., Czymmek, K., and Valent, B. 2007. Roles for rice membrane dynamics and plasmodesmata during biotrophic invasion by the blast fungus. *Plant Cell* **19**, 706–724.

Kanungo, A. and Prasad, B. 2019. Structural insights into the molecular mechanisms of pectinolytic enzymes. *J. Proteins Proteom.* **10**, 325–344.

Keegstra, K. 2010. Plant cell walls. *Plant Physiol.* **154**, 483–486.

Leisen, T., Bietz, F., Werner, J., Wegner, A., Schaffrath, U., Scheuring, D., Willmund, F., Mosbach, A., Scalliet, G., and Hahn, M. 2020. CRISPR/Cas with ribonucleoprotein complexes and transiently selected telomere vectors allows highly efficient marker-free and multiple genome editing in *Botrytis cinerea*. *PLoS Pathog.* **16**, e1008326.

Levy, A., Salas Gonzalez, I., Mittelviefhaus, M., Clingenpeel, S., Herrera Paredes, S., Miao, J., Wang, K., Devescovi, G., Stillman, K., Monteiro, F., *et al.* 2018. Genomic features of bacterial adaptation to plants. *Nat. Genet.* **50**, 138–150.

Livak, K.J. and Schmittgen, T.D. 2001. Analysis of relative gene expression data using real-time quantitative PCR and the $2^{-\Delta\Delta CT}$ method. *Methods* **25**, 402–408.

Loehrer, M., Botterweck, J., Jahnke, J., Mahlmann, D.M., Gaetgens, J., Oldiges, M., Horbach, R., Deising, H., and Schaffrath, U. 2014. *In vivo* assessment by Mach-Zehnder double-beam interferometry of the invasive force exerted by the Asian soybean rust fungus (*Phakopsora pachyrhizi*). *New Phytol.* **203**, 620–631.

Miyara, I., Shafran, H., Kramer Haimovich, H., Rollins, J., Sherman, A., and Prusky, D. 2008. Multi-factor regulation of pectate lyase secretion by *Colletotrichum gloeosporioides* pathogenic on avocado fruits. *Mol. Plant Pathol.* **9**, 281–291.

Mogga, V., Delventhal, R., Weidenbach, D., Langer, S., Bertram, P.M., Andresen, K., Thines, E., Kroj, T., and Schaffrath, U. 2016. *Magnaporthe oryzae* effectors MoHEG13 and MoHEG16 interfere with host infection and MoHEG13 counteracts cell death caused by *Magnaporthe*-NLPs in tobacco. *Plant Cell Rep.* **35**, 1169–1185.

Mori, T., Jung, H.Y., Maejima, K., Hirata, H., Himeno, M., Hamamoto, H., and Namba, S. 2008. *Magnaporthe oryzae* endopolygalacturonase homolog correlates with density-dependent conidial germination. *FEMS Microbiol. Lett.* **280**, 182–188.

Quoc, N.B. and Chau, N.N. 2017. The role of cell wall degrading enzymes in pathogenesis of *Magnaporthe oryzae*. *Curr. Protein Pept. Sci.* **18**, 1019–1034.

Saitoh, H., Fujisawa, S., Mitsuoka, C., Ito, A., Hirabuchi, A., Ikeda, K., Irieda, H., Yoshino, K., Yoshida, K., Matsumura, H., *et al.* 2012. Large-scale gene disruption in *Magnaporthe oryzae* identifies MC69, a secreted protein required for infection by monocot and dicot fungal pathogens. *PLoS Pathog.* **8**, e1002711.

Shimizu, M., Nakano, Y., Hirabuchi, A., Yoshino, K., Kobayashi, M., Yamamoto, K., Terauchi, R., and Saitoh, H. 2019. RNA-Seq of in planta-expressed *Magnaporthe oryzae* genes identifies MoSVP as a highly expressed gene required for pathogenicity at the initial stage of infection. *Mol. Plant Pathol.* **20**, 1682–1695.

Skamnioti, P. and Gurr, S.J. 2007. *Magnaporthe grisea* cutinase2 mediates appressorium differentiation and host penetration and is required for full virulence. *Plant Cell* **19**, 2674–2689.

Talbot, N.J. 2003. On the trail of a cereal killer: exploring the biology of *Magnaporthe grisea*. *Annu. Rev. Microbiol.* **57**, 177–202.

Underwood, W. 2012. The plant cell wall: a dynamic barrier against pathogen invasion. *Front. Plant Sci.* **3**, 85.

van den Brink, J. and de Vries, R.P. 2011. Fungal enzyme sets for plant polysaccharide degradation. *Appl. Microbiol. Biotechnol.* **91**, 1477–1492.

Voegele, R.T. and Schmid, A. 2011. RT real-time PCR-based quantification of *Uromyces fabae in planta*. *FEMS Microbiol. Lett.* **322**, 131–137.

Wilson, R.A. and Talbot, N.J. 2009. Under pressure: investigating the biology of plant infection by *Magnaporthe oryzae*. *Nat. Rev. Microbiol.* **7**, 185–195.

Yakoby, N., Kobiler, I., Dinoor, A., and Prusky, D. 2000. pH regulation of pectate lyase secretion modulates the attack of *Colletotrichum gloeosporioides* on avocado fruits. *Appl. Environ. Microbiol.* **66**, 1026–1030.

Yoder, M.D., Keen, N.T., and Jurnak, F. 1993. New domain motif: the structure of pectate lyase C, a secreted plant virulence factor. *Science* **260**, 1503–1507.

Yoshida, K., Saitoh, H., Fujisawa, S., Kanzaki, H., Matsumura, H., Yoshida, K., Tosa, Y., Chuma, I., Takano, Y., Win, J., *et al.* 2009. Association genetics reveals three novel avirulence genes from the rice blast fungal pathogen *Magnaporthe oryzae*. *Plant Cell* **21**, 1573–1591.

Zheng, X., Zhou, J., Lin, X., Lan, L., Wang, Z., and Lu, G. 2009. Secretion property and gene expression pattern of a putative feruloyl esterase in *Magnaporthe grisea*. In Wang, G.L. and Valent, B. (eds.) Advances in Genetics, Genomics and Control of Rice Blast Disease. Springer, Dordrecht, Netherlands.